Ann. Phys. (Berlin) **17**, No. 12, 922 – 936 (2008) / **DOI** 10.1002/andp.200810326

DMRG studies of critical SU(N) spin chains

Max Führinger[1], **Stephan Rachel**[1,*], **Ronny Thomale**[1], **Martin Greiter**[1], and **Peter Schmitteckert**[2]

[1] Institut für Theorie der Kondensierten Materie, Universität Karlsruhe, 76128 Karlsruhe, Germany
[2] Institut für Nanotechnologie, Forschungszentrum Karlsruhe, 76021 Karlsruhe, Germany

Received 16 June 2008, revised 8 August 2008, accepted 20 August 2008 by U. Eckern
Published online 20 October 2008

Key words Integrable spin Hamiltonian, DMRG, SU(N) spin models.
PACS 02.30.Ik, 11.25.Hf, 75.10.Jm

The DMRG method is applied to integrable models of antiferromagnetic spin chains for fundamental and higher representations of SU(2), SU(3), and SU(4). From the low energy spectrum and the entanglement entropy, we compute the central charge and the primary field scaling dimensions. These parameters allow us to identify uniquely the Wess–Zumino–Witten models capturing the low energy sectors of the models we consider.

With the rise of quantum mechanics in the late 20's of the last century [1,2], quantum magnetism emerged as a predominant area of research in theoretical condensed matter physics. This was to a significant part induced by the notion of the electron spin, i.e., the magnetically sensitive, internal degree of freedom of electrons, in the early 20's, which rendered the classical picture insufficient. In contrast to orbital angular momentum, which is quantized in integer units of $\hbar$ in accordance with the spatial rotation group SO(3), the internal spin is in accordance with the Lie group SU(2) quantized in integer units of $\hbar$ (the generators of both groups are identical as SU(2) is locally isomorphic to SO(3)). Ever since the invention of the Bethe ansatz in 1931 as a method to solve the $S = 1/2$ Heisenberg chain with nearest-neighbor interactions [3], spin models in (1+1) dimension, i.e., quantum spin chains, have been a most rewarding subject of study. Bethe's work eventually led to the discovery of the Yang-Baxter equation in 1967 [4] and provides the foundation of the field of integrable models. The notion of integrability rendered a plethora of models amenable to exact and often rather explicit solution [5,6]. Quantum spin chains possess rich and deeply complex physical properties. For example, it took several decades until Faddeev and Takhtajan [7] discovered in 1981 that the elementary excitations of the $S = 1/2$ Heisenberg chain solved by Bethe carry spin $1/2$ and not, as previously assumed, spin 1. The excitations of the spin $1/2$ chain hence provide an instance of fractional quantization, as the Hilbert space for the chain is spanned by spin flips, which carry spin 1.

Several new aspects, both phenomenological and technical, emerge when the spins transform under higher representations of SU(2). In particular, Haldane proposed in 1983 that half-integer spin chains are generically gapless, whereas integer spin chains possess a gap in the excitation spectrum [8–11]. This leads to strikingly different behavior in the magnetic susceptibility at low temperatures. A gap leads to exponentially decaying spin-spin correlations and as such to a vanishing susceptibility at temperature $T = 0$. In contrast, a gapless spectrum is generically associated with correlations which decay as a power law with the distance, and a finite susceptibility at low temperatures. Haldane's at that time astonishing prediction was confirmed experimentally in $S = 1$ chains [12–14].

Yet another generalization of quantum spin chains is to enlarge the spin symmetry group from SU(2) to SU(N) [15]. Among those, the group SU(3) plays a special role, as both color and flavor symmetries in particle physics provide instances. As the electron spin transforms according to the fundamental (up/down)

* Corresponding author E-mail: rachel@tkm.uni-karlsruhe.de

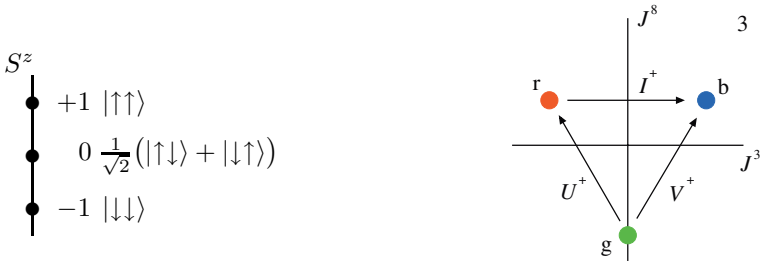

a) Spin 1 representation of SU(2) b) Fundamental representation of SU(3)

Fig. 1 (online colour at: www.ann-phys.org) a) Weight diagram of the three-dimensional spin $S = 1$ representation of SU(2). The SU(2) weight diagrams are one–dimensional since there is only one diagonal generator (S^z) in the group SU(2). There is only one raising operator (S^+) and one lowering operator (S^-) and, hence, there is no generator connecting the $S^z = -1$ and the $S^Z = +1$ state directly. b) Weight diagram of the three–dimensional, fundamental representation of SU(3). SU(3) weight diagrams are two–dimensional since both J^3 and J^8 are diagonal generators of the group SU(3). Due to the higher dimensionality of SU(3), each point in the weight diagram is directly connected with each other by the raising and lowering operators I^+, I^-, U^+, U^-, V^+, and V^-, as illustrated in the diagram.

doublet representation of SU(2), an internal "color" degree of freedom of quarks transforms according to the three dimensional fundamental representation of SU(3), and thus can be assigned a quantum number taking the values blue, red, and green.

In the not-to distant future, it might be possible to realize SU(3) spin chains in optical lattices of ultra-cold atoms [16]. There, one important challenge of the implementation is that the system of the distinct atomic states corresponding to blue, red, and green must be tuned in such a way that the pairwise transition weights are equal, as the system only then correctly resembles the SU(3) spin algebra with six raising/lowering operators I^+, I^-, U^+, U^-, V^+, and V^- linking the states of the fundamental representation with each other (Fig 1b). From this perspective, it becomes immediately obvious that this is completely different from a three-dimensional $S = 1$ representation of SU(2), where the raising and lowering operators S^+ and S^- map the $S^z = 0$ state to $S^z = \pm 1$, while there is no direct transition from $S^z = -1$ to $S^z = +1$ and vice versa (Fig. 1a). It has also been proposed that for approximately implemented SU(N) chains of N-component fermions, a molecular superfluid phase may appear [17]. Recently, SU(4) spin chains attracted experimental interest in the field of transition-metal and rare earth compounds, where such models appear to capture the physics of coupled electronic and orbital degrees of freedom [18, 19].

From a field theoretical point of view, conformal field theories (CFTs) have been enormously successful in describing the low energy behavior of critical SU(N) spin chains [20–22]. In this framework, critical means that the spins of the chain have a diverging correlation length related to a gapless spectrum, corresponding to the scale or, more precisely, conformal invariance of the effective field theory describing these systems [23]. The Wess-Zumino-Witten model (WZW) plays a crucial role among those models [24, 25].

Criticality is intimately related to the integrability of the SU(N) spin chain models which we study in this article. For the fundamental representations of SU(2), SU(3), and SU(4), as well as higher representations of SU(2) and SU(3), we numerically investigate integrable models and their related CFTs, i.e., the SU(N) WZW models of different levels k. The Density Matrix Renormalization Group (DMRG) method provides us with a highly suitable numerical method to study the low energy sector of spin chains [26–29]. From the results of our DMRG studies, we extract the central charge and scaling dimension. These parameters specify the associated effective field theory. We thus endeavor to establish numerically the correspondence between CFTs and SU(N) spin chains.

This article is organized as follows. In Sect. 1, we briefly review the basic features of CFT relevant to our considerations, i.e., the scaling dimension and the central charge. The DMRG approach to SU(N) spin chains

is discussed in Sect. 2. In particular, we explain the implementation of the SU(N) spin algebra with its N^2-1 generators and discuss the problem of convergence as N is increased. In Sect. 3, we introduce the integrable models we consider. These include the nearest neighbor Heisenberg Hamiltonian for the fundamental representations of SU(2), SU(3), and SU(4), as well as the integrable Takhtajan–Babudjan Hamiltonians for $S = 1$ and $S = 3/2$ [30–32]. We also perform DMRG studies of the integrable SU(3) model with spins transforming under the higher representation **6** proposed by Andrei and Johanneson [33, 34]. The numerical results are presented in Sect. 4, and used to extract the central charge and scaling dimension of the corresponding WZW models. In Sect. 5, we conclude that the DMRG method can be successfully applied to study SU(N) spin chains.

1 Conformal field theory, the central charge and scaling invariance

The SU(N) Wess–Zumino–Witten (WZW) models have been found to capture the low energy behavior of a family of critical quantum spin chains [20]. WZW models are conformal field theories, meaning that the Lagrangians are invariant under conformal mappings. These are all combinations of translation, rotation, and dilatation in two–dimensional space-time. For field theories with conformal invariance, it suffices to specify the scaling of the fields or rather the scaling of their correlation functions to characterize the theory completely [23]. As such, once a CFT is identified, there is no immediate need to work with the associated Lagrangian. Our emphasis in this article will be on the relation between the universal parameters of the CFT and numerically accessible measures, which we extract from the DMRG studies of the corresponding spin chain models. As a general structure, a WZW model consists of a non-linear sigma model term and k times a topological Wess-Zumino term, where k is a non-zero positive integer [23]. The SU(N) WZW model of level k (denoted SU$(N)_k$ WZW in the following) can be characterized by the central charge and the scaling dimension of the primary field, both of which we will evaluate numerically in Sect. 4 below. In the following formulas, subleading finite size contributions are neglected if they appear.

1.1 Central charge

The central charge c is defined in the framework of the Virasoro algebra of the CFT [23]. Alternatively, c is also named conformal anomaly number. It appears in the correlation function of the energy momentum tensor $T(z)$ of the theory, where z denotes a complex space-time variable. This correlation has a singularity as $z \to 0$, with a prefactor proportional to c, $\langle T(z)T(0)\rangle \sim \frac{c/2}{z^4}$. For the SU$(N)_k$ WZW, c is given by

$$c = \frac{k(N^2-1)}{k+N}. \tag{1}$$

The for our purposes relevant feature of the central charge is that c appears as a universal scaling factor in the microscopically accessible entanglement entropy [35]. Let i denote a site, L the total length of the spin chain, $i = 1, \ldots, L$, and ρ_α the reduced density matrix where all the degrees of freedom on sites $i > \alpha$ are traced out, i.e., $\rho_\alpha = \mathrm{Tr}_{i>\alpha}\rho$. For this case, the entanglement entropy is given by

$$S_{\alpha,L} = -\mathrm{Tr}\big[\rho_\alpha \log \rho_\alpha\big]. \tag{2}$$

For periodic boundary conditions and central charge c, the entropy then takes the form [36]

$$S_{\alpha,L} = \frac{c}{3}\log\left[\left(\frac{L}{\pi}\right)\sin\left(\frac{\pi\alpha}{L}\right)\right] + c_1, \tag{3}$$

where c_1 is a non-universal constant and the lattice spacing is set to unity. Thus, with L being the total number of sites divided by unit lattice spacing, the entanglement entropy obeys the symmetry relation $S_{\alpha,L} = S_{L-\alpha,L}$ and has its maximum at $\alpha = L/2$. By virtue of (3), c can be extracted directly from the entanglement entropy calculated via DMRG.

1.2 Scaling dimension

The scaling dimension x is a property of the fields ϕ of the CFT [37]. Conformal invariance implies that the two-point correlation function of the field must satisfy

$$\langle\phi(z_1)\phi(z_2)\rangle = |f'(z_1)|^x |f'(z_2)|^x \langle\phi(f(z_1))\phi(f(z_2))\rangle, \tag{4}$$

where we constrain the conformal mapping $f(z)$ to a dilatation, and $f'(z)$ is its derivative at point z. For the finite systems we study numerically, we can use that the low energy spectrum, and hence the energies of the finite system, can be classified by the associated CFTs. The lowest excited states (labeled by p) above the ground state ($p = 0$) belong spectrally to a conformal tower [38], with energies which obey the relation

$$E_{p,L} - E_{0,L} = \frac{2\pi v}{L} x_p, \tag{5}$$

where x_p denotes the scaling dimension of the field associated with the pth state, and v is the Fermi velocity. The dependence on v reflects that in the low energy limit, the only relevant momentum scale of the spin chain is provided by the linearized dispersion around the Fermi points. This allows us to extract the scaling dimension times the Fermi velocity, $x_p v$, as the energies in the l.h.s. of (5) are numerically accessible through DMRG. In the following, we shall focus on the first excited state $x_1 \equiv x$, i.e., the scaling dimension of the primary field.

1.3 Fermi velocity parameter

In view of (3) and (5), it is clear that we need one further relation, to extract the Fermi velocity v from our numerical studies. The required relation is

$$E_{0,L} = E_{0,\infty} - \frac{\pi c v}{6L}, \tag{6}$$

where $E_{0,L}$ and $E_{0,\infty}$ denote the ground state energies of the finite and the infinite chain, respectively. This relation can be easily understood from the field theoretical point of view [38]: For a finite length and temperature $T = 0$, L sets the inverse energy scale of the system. This scale can be rephrased in terms of a field theory at finite temperature and no length scale, i.e., an infinite chain at temperature $T = v/L$.

Writing (6) in terms of the free energy density for this finite temperature field theory, we obtain the correct specific heat linear in T, as we expect for a gapless spectrum. As we calculate $E_{0,L}$ directly and extract $e_{0,\infty} = E_{0,L}/L$ for $L \to \infty$ by finite size scaling, we can obtain v from (6) once we have obtained c from (3).

2 The DMRG method

In the last decade, the DMRG was successfully applied to numerous SU(2) spin models. Very recently, the DMRG was further used to investigate the SU(3) representation **3** Heisenberg model [39]. Here we generalize to the six–dimensional representation $(2, 0) \equiv \mathbf{6}$ of SU(3), which is formed by symmetric combination of two fundamental representations of SU(3). We also present DMRG studies of a spin chain with spins transforming under the fundamental representation of SU(4). Our work hence requires the explicit implementation of the su(3) and su(4) spin algebras with its $N^2 - 1$ generators, which are explicitly given in Apps. B and C. Note that this implementation is more involved than the implementation of SU(N) Hubbard models, where the explicit spin algebra does not enter, and the SU(N) symmetry enters only through the number of different fermionic species.

An important problem with numerical studies of SU(N) spin chains in general is the increasing dimensionality of the subspace of one site of the chain, due to either larger values for N or higher spin representations (like rep **6** for SU(3)). For DMRG, of course, this dimensionality limits the system sizes we

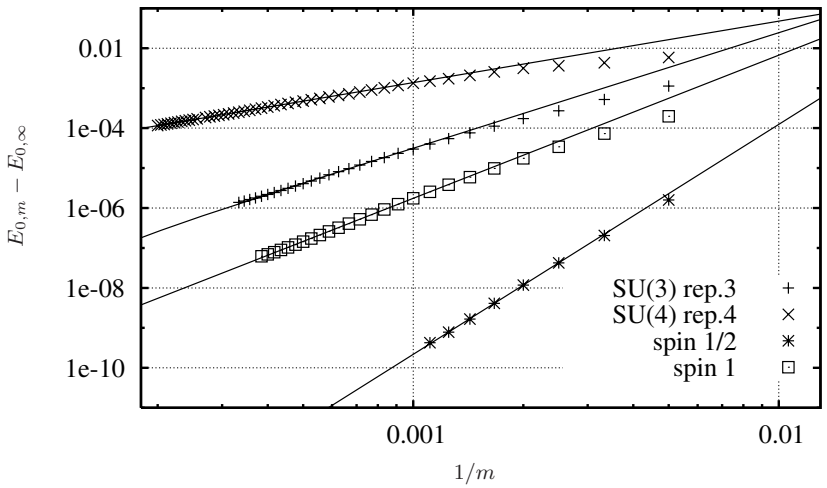

Fig. 2 Periodic Boundary Conditions: logarithmic plot for the energy difference of the finite size ground state energy and the thermodynamic site limit $L \to \infty$ versus inverse number of states m kept in the DMRG sweeps. Shown are the lines for the nearest neighbor Heisenberg model in the fundamental representations of SU(2), SU(3), and SU(4), as well as for the $S = 1$ TB model for comparison. The length of the chain is $L = 48$.

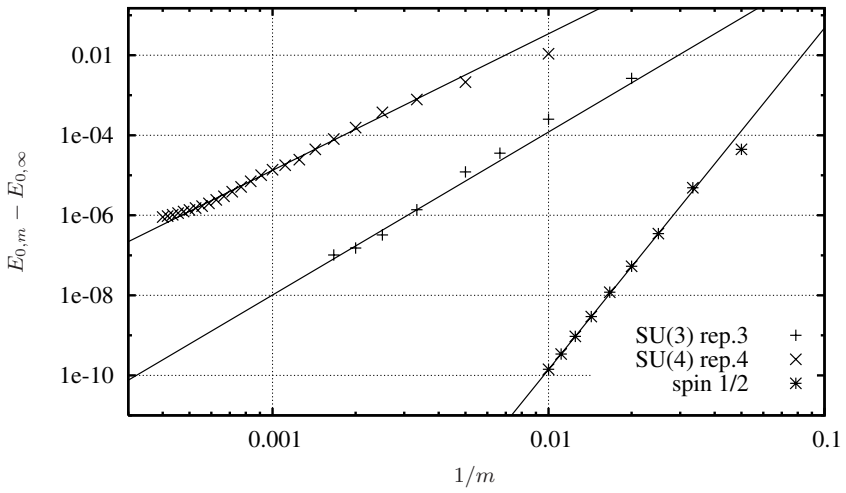

Fig. 3 Hard Wall Boundary Conditions: logarithmic plot for the energy difference of the finite size ground state energy and the thermodynamic limit $L \to \infty$ versus inverse number of states m kept in the DMRG sweeps. Shown are the lines for the fundamental representations of SU(2), SU(3), and SU(4). The length of the chain is again $L = 48$. As compared to the case of PBCs shown in Fig. 2, the system converges much faster for a comparable number of states kept in the DMRG sweeps.

can access. In Fig. 2, we have plotted the convergence of the DMRG iteration as the number m of states kept in the effective density matrix is increased. We observe that for comparable m, the convergence decreases rapidly as we go to higher SU(N), according for the exponential increase of the Hilbert space as the number of states per site grows. However, as confirmed by our numerical results reported below, our DMRG code is capable of at least handling critical spin chains up to SU(4) with reasonable convergence and accuracy.

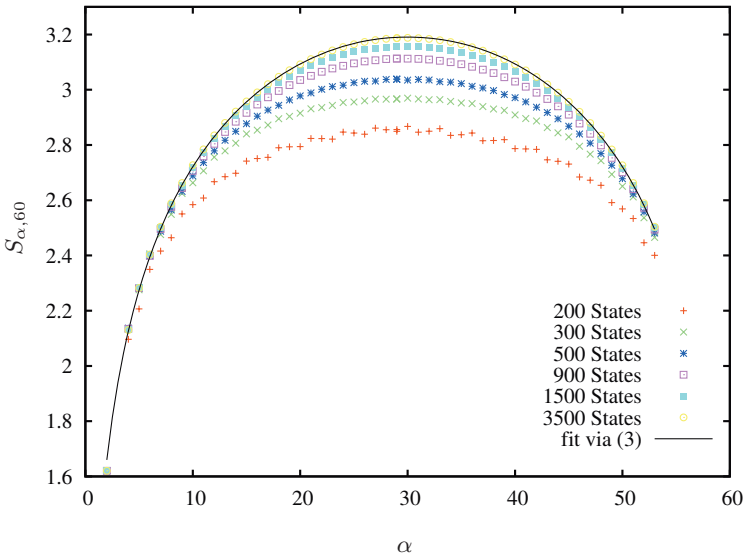

Fig. 4 (online colour at: www.ann-phys.org) The entanglement entropy $S_{\alpha,60}$ as another example for the convergence behavior of the SU(3) Heisenberg model. (a) shows the EE $S_{\alpha,60}$. The different curves correspond to different number of kept DMRG states (200, 300, 500, 900, 1500, 3500 states). The system with 3500 kept DMRG states is fully converged and provides a benchmark. The truncated Hilbert space for this converged job contains about 8 million states.

While the plots in Fig. 2 are obtained using periodic boundary conditions (PBCs), the convergence behavior for hard wall boundary conditions (HWBCs) is shown in Fig. 3. Note that HWBCs rather than PBCs are the natural choice for DMRG, as the number of DMRG states m we need to keep to achieve a similar level of precision for PBCs is, according to our calculations, roughly the square of the number of states we need to keep for HWBCs. Nonetheless, the results we present below are obtained with PBCs, as PBCs allow a more convenient treatment of the finite size corrections for the quantities we extract. In particular, (6) is valid only for PBCs. (There is a relation corresponding to (3) for HWBCs [36].) We have used 10 DMRG sweeps for all the calculations we present.

As a demonstration of convergence, Fig. 4 shows the entanglement entropy for different numbers of kept DMRG states m for the SU(3) representation **3** Heisenberg model. The result displays the $S_{\alpha,L} = S_{L-\alpha,L}$ symmetry mentioned above and fits the prediction (3) to astonishing accuracy. We find, however, that this accuracy requires a number m of states kept which is large in comparison with standard applications of the DMRG method, and which demands large computational resources. This is partially due to the criticality of the models we study. With a spectrum that is gapless in the thermodynamic limit, a large subspace of the entire Hilbert space contributes to the long range correlations, which is reflected in a large number of relevant weights in the density matrix. Nonetheless, with a sufficiently high value of states kept, very accurate results can be extracted from the DMRG computations. Even for rather small systems consisting of $\mathcal{O}(100)$ sites, we obtain highly accurate estimates for the central charges of the critical models described in the following section. As the entanglement entropy is not directly accessible by other numerical methods, the DMRG method is preeminent to our purposes.

3 Integrable models of critical SU(N) chains

The SU(N) spin chain models we investigate numerically in this work are described by a family of Hamiltonians $\mathcal{H}^{[N,m]}$, which are amenable to the transfer matrix method [30–34, 40]. Note that some of the models

$\mathcal{H}^{[N,m]}$ were investigated by numerical and analytical solutions of the Bethe ansatz equations [41–43]. The representations $[N, m]$ of SU(N) are given by the totally symmetric combination of m fundamental representations of SU(N). The corresponding Young tableaux is

For SU(2), all the representations are of this form, with $m = 2S$. For SU(3), the symmetric representations include the fundamental representation **3** and the representation **6**, for $m = 1$ and 2, respectively. The dimensionality n of the totally symmetric representation $[N, m]$ is in general given by

$$n \equiv \dim[N, m] = \binom{N-1+m}{m}. \tag{7}$$

The Hamiltonians $\mathcal{H}^{[N,m]}$ contain two-site interactions only and are invariant under global SU(N) spin rotations, i.e., Heisenberg interaction terms to arbitrary power [30–34,40]. Note that all the models $\mathcal{H}^{[N,m]}$ are integrable, due to an infinite number of operators which commute with the Hamiltonians. In this work, we consider the models with $[N, m] = [2, 1]$, $[2, 2]$, $[2, 3]$, $[3, 1]$, $[3, 2]$, and $[4, 1]$.

The Hamiltonians for $[N, 1]$, i.e., the fundamental representations, are just the nearest-neighbor Heisenberg models,

$$\mathcal{H}^{[N,1]} = \sum_{i=1}^{\mathcal{N}} \boldsymbol{S}_i \boldsymbol{S}_{i+1}. \tag{8}$$

In general, $\boldsymbol{S}_i$ is an SU(N) representation $[N, m]$ spin operator at site i. Since the dimension of the Lie algebra su(N) is $N^2 - 1$, the spin operator $\boldsymbol{S}_i$ consists of the $N^2 - 1$ generators,

$$S_i^\alpha = \frac{1}{2} \sum_{\sigma,\sigma'=f_1,\ldots,f_n} c_{i\sigma}^\dagger V_{\sigma\sigma'}^\alpha c_{i\sigma'}, \tag{9}$$

where $\alpha = 1, \ldots, N^2 - 1$, $V_{\sigma\sigma'}^\alpha$ are the SU(N) Gell-Mann matrices, and $f_1, \ldots, f_n$ denote the n different spin states [15]. Trivially, $\boldsymbol{S}_i \boldsymbol{S}_{i+1} \equiv \sum_{\alpha=1}^{N^2-1} S_i^\alpha S_{i+1}^\alpha$.

For the fundamental representation $[2, 1]$ of SU(2), the V's are just the Pauli matrices and the two spin states can be classified by the eigenstates $f_1 = \uparrow$, $f_2 = \downarrow$ of S^z. For the fundamental representation $[3, 1]$ of SU(3), the V's are given by the eight Gell-Mann matrices. The matrices V for representations $[3, 2]$ (i.e., SU(3) representation **6**) and $[4, 1]$ (i.e., SU(4) representation **4**) are written out in Apps. B and C. In our numerical implementations, we have scaled the Hamiltonians such that the pre-factor of the bilinear Heisenberg term $\boldsymbol{S}_i \boldsymbol{S}_{i+1}$ is ± 1 and we have dropped the constant term.

As we confirm numerically below, the low-energy behavior of the models $\mathcal{H}^{[N,1]}$ is described by the SU(N)$_1$ WZW model, with topological coupling constant $k = 1$. With (1), we expect to find $c = N - 1$ for the central charge. The integrable spin $S = 1$ model we investigate, the Takhtajan–Babudjan model [30–32], is given by

$$\mathcal{H}^{[2,2]} = \sum_{i=1}^{\mathcal{N}} \left[\boldsymbol{S}_i \boldsymbol{S}_{i+1} - (\boldsymbol{S}_i \boldsymbol{S}_{i+1})^2 \right]. \tag{10}$$

The low energy physics is described by the SU(2)$_2$ WZW model. With (1), we expect to find $c = \frac{3}{2}$. Note that the criticality of this integer spin model is not inconsistent with the Haldane gap, as Haldane's

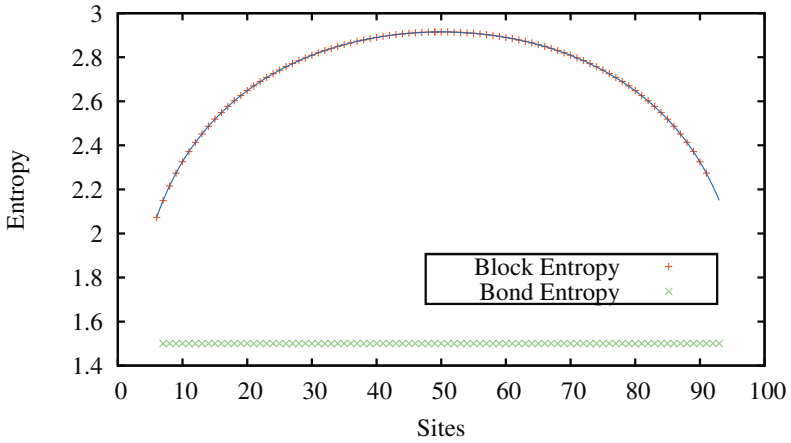

Fig. 5 (online colour at: www.ann-phys.org) Entanglement entropy (block entropy) of the integrable SU(2) $S = 1$ Hamiltonian with PBCs. The solid line corresponds to the formula (3) with the fit parameter c, the central charge of the corresponding CFT. The uniform bond entropy, i.e., the nearest neighbor entanglement entropy, indicates a homogeneous and translationally invariant ground state.

classification applies to *generic* integer spin chains, while the Takhtajan–Babudjan model (10) is tuned to criticality.

The next higher dimensional integrable SU(2) model from the Takhtajan–Babudjan series is given by the spin 3/2 Hamiltonian

$$\mathcal{H}^{[2,3]} = \sum_{i=1}^{\mathcal{N}} \left[-\boldsymbol{S}_i \boldsymbol{S}_{i+1} + \frac{8}{27} \left(\boldsymbol{S}_i \boldsymbol{S}_{i+1} \right)^2 + \frac{16}{27} \left(\boldsymbol{S}_i \boldsymbol{S}_{i+1} \right)^3 \right]. \tag{11}$$

The corresponding CFT is the $SU(2)_3$ WZW model, which implies that the central charge is $c = \frac{9}{5}$.

Finally, the Andrei–Johannesson [33, 34] model consists of SU(3) spins transforming under the six–dimensional representation **6**, and is given by

$$\mathcal{H}^{[3,2]} = \sum_{i=1}^{\mathcal{N}} \left[\boldsymbol{S}_i \boldsymbol{S}_{i+1} - \frac{3}{5} \left(\boldsymbol{S}_i \boldsymbol{S}_{i+1} \right)^2 \right]. \tag{12}$$

The corresponding CFT is the $SU(3)_2$ WZW model, which implies $c = \frac{16}{5}$. We now turn to our numerical results for these models.

4 Numerical results

4.1 Central charge

As noted above, the entanglement entropy is provided quite naturally in DMRG, as in each sweep we really calculate reduced density matrices, from which we easily obtain the entanglement entropy via (2). From the plots of the entanglement entropy vs. the site index, we obtain a numerical value for the central charge via (3). In Fig. 5, we show the entanglement entropy (also called block entropy) for the integrable $S = 1$ Hamiltonian, the Takhtajan–Babudjan model, as an illustrative example. The fit yields a central charge of $c = 1.50717 \pm 0.0003$, where the error corresponds to the fitting error shown in Table 1. The result is in excellent agreement with the value $c = \frac{3}{2}$ predicted by CFT. We have also plotted the bond entropy, which is the entanglement entropy of two neighboring sites α and $\alpha + 1$ with the remainder of the system. In

Table 1 Theoretical predictions and numerical results for the central charge for the Hamiltonians we considered. The error quoted are due to inaccuracies when fitting the data for entanglement entropy obtained numerically to (3). An additional systematic error, which we have not estimated separately, arises from the states discarded within the DMRG.

Hamiltonian $[N, m]$	N	k	c	c_{DMRG}
$[2, 1]$	2	1	1	1.0001 ± 0.0012
$[2, 2]$	2	2	$\frac{3}{2}$	1.5072 ± 0.0003
$[2, 3]$	2	3	$\frac{9}{5}$	1.8002 ± 0.0211
$[3, 1]$	3	1	2	2.0001 ± 0.0102
$[3, 2]$	3	2	$\frac{16}{5}$	3.2214 ± 0.0437
$[4, 1]$	4	1	3	2.9527 ± 0.0237

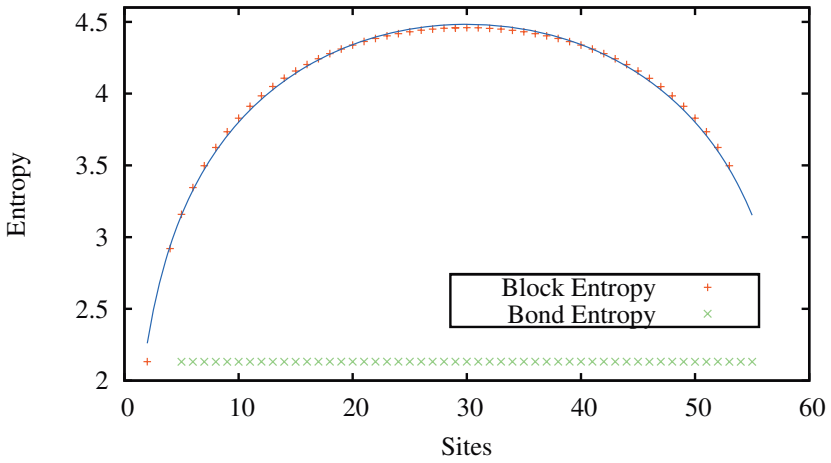

Fig. 6 (online colour at: www.ann-phys.org) Entanglement entropy (block entropy) of the SU(4) nearest neighbor Heisenberg model with PBCs. The solid line constitutes a fit of the data using (3), yielding a central charge close to the predicted value $c = 3$ (for details see Table 1).

general, a bond entropy which is not site independent indicates a spontaneous breakdown of translational invariance (like e.g. dimerization) in the ground state. Despite being a quantity of its own interest to extract information from finite systems [44], we attach no significance to the bond entropy beyond the confirmation of translational invariance. Other quantities, e.g. the ground state stiffness [45], could in principle be studied within DMRG to supplement the ground state studies, but are not our point of consideration in this work.

The discrepancy between the data and the fit to (3) is most visible at the maximum of the entanglement entropy, i.e., for half of the sites traced out, as this discrepancy is due to entropy we have discarded by discarding states. While there is no difference visible in Fig. 5, a discrepancy can be discerned in Fig. 6, where we have plotted the entanglement entropy of the SU(4) Heisenberg model in the fundamental representation. This small discrepancy is present even though we keep 8000 DMRG states for the sweep iterations which results in a truncated Hilbert space containing 22 million states. Note that the DMRG calculation for the ground state of this model with 8000 kept states has taken 68 hours of computer time (4 CPU cores) with ca. 20 gigabyte of memory, while the same calculation with 5500 kept states has taken 28 hours (4 CPU cores) with ca. 9 gigabyte of memory. Here we only exploited the abelian quantum numbers of SU(N). By using

the square of the total spin $\boldsymbol{S}^2$ as additional quantum number and representing the states according to the Wigner–Eckhardt theorem, one should be able to reduce the required Hilbert space significantly. However, already for SU(2), the Clebsch–Gordon coefficients make the implementation cumbersome [46], and for SU(3) and SU(4) the corresponding Clebsch–Gordon coefficients are more complicated. Therefore we decided not to implement them. Note that the use of non–abelian quantum numbers does not automatically lead to better performance, e.g. in SU(2) it helps for small S sectors only, since otherwise the sum over reduced states gets too involved.

The value we obtain for the central charge, $c = 2.95268 \pm 0.02368$, however, is reasonably close to the predicted value $c = 3$. In addition to the fitting error we quote in Table 1, there is a systematic error due to the entropy we have discarded by discarding states in DMRG. As all the contributions to the entanglement entropy are positive definite, this systematic error leads to a slight underestimate for the numerically obtained central charge. Our results for the models introduced in Sect. 3 are presented in Table 1. In general, we find excellent agreement between analytical values and numerical data.

4.2 Scaling dimension of critical models

From the spectrum we numerically calculate via DMRG, it takes two steps to obtain an estimate for the scaling dimension of the primary field. First, with the central charge obtained through the entanglement entropy, we use (6) to arrive at an estimate for the Fermi velocity v. Second, we use (5) to obtain an approximate value for the scaling dimension x. The values we obtain for some of the models we study are listed in Table 2.

Both steps require only linear fits, which are easily accomplished. For the fundamental representations of SU(2) and SU(3), these fits are shown in Figs. 7 and 8. In the process, however, we omit significant finite size corrections. To begin with, in (6), marginal sub-leading contributions of the order of $\mathcal{O}(\frac{1}{L(\log L)^3})$ are omitted [47]. As we consider spin chains with of the order of 100 sites, these corrections are at the order of 1% and thus for our purposes negligible. In (5), however, the error due to omitting marginal contributions is of order $\mathcal{O}(\frac{1}{L \log L})$, and hence significantly larger. This error is essentially responsible for the discrepancy between the analytical results and the numerical findings in Table 2. For these reasons, our numerical results for the scaling dimension are not nearly as accurate as for the central charges, where finite size corrections did not enter. By use of non-Abelian bosonization [38], the logarithmic correction can be calculated in principle. For the case $S = 1$ of SU(2), this has been carried out by Hijii and Nomura [48]. For our purposes, however, such an analysis is not required. The fits to leading order for the cases $S = 1/2$ and $S = 1$ of SU(2) as well as the fundamental representation **3** of SU(3) are sufficiently conclusive to identify the scaling dimension of the primary fields of the corresponding WZW model. For a more refined spectral analysis or calculation of the various scaling dimensions of the descendants of the primary fields, however, it would be indispensable to include the marginal contributions into the fits as well.

Table 2 Theoretical predictions and numerical results for the scaling dimension of the primary fields for SU(2) and SU(3) Hamiltonians. The deviations from the analytical values are higher than the deviations for central charges discussed above. The errors quoted again refer to inaccuracies of the fits only.

Hamiltonian $[N, m]$	N	k	x	x_{DMRG}
$[2, 1]$	2	1	$\frac{1}{2}$	0.443 ± 0.0020
$[2, 2]$	2	2	$\frac{3}{8}$	0.338 ± 0.0006
$[3, 1]$	3	1	$\frac{2}{3}$	0.638 ± 0.0010

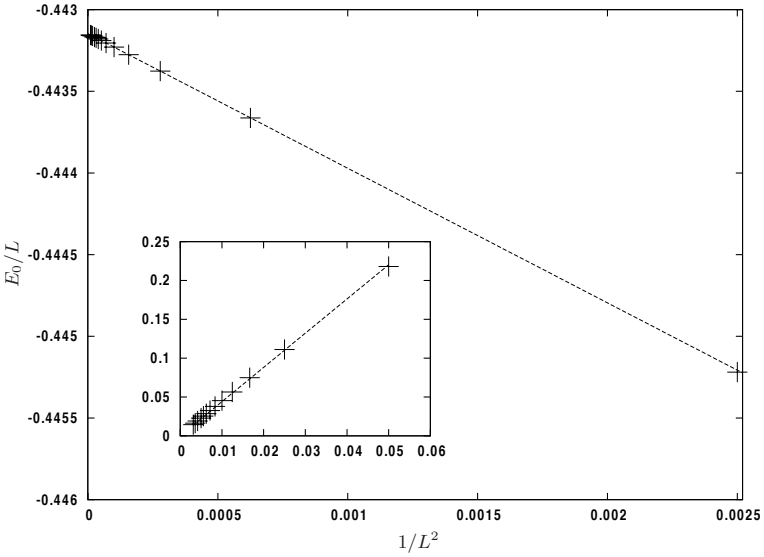

Fig. 7 Scaling dimension for the spin 1/2 Heisenberg model. According to Eq. (6) the Fermi velocity is fitted in the main picture ($v \sim \frac{\pi}{2}$), which is used as a parameter for the fit of the scaling dimension done in the inset. In the inset, $E_{1,L} - E_{0,L}$ is plotted vs. $1/L$ and according to Eq. (5) we have fitted the scaling dimension $x = 0.443 \pm 0.0020$. The data points correspond to chains (PBCs) from 20 to 320 sites.

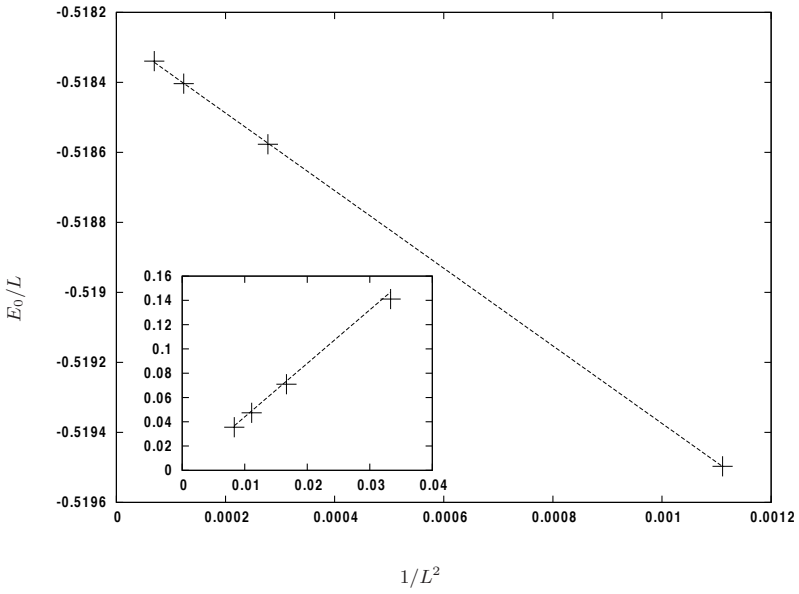

Fig. 8 Scaling dimension for the SU(3) representation **3** Heisenberg model. Less data points have been computed compared to $S = 1/2$ SU(2) in Fig. 7, but yields a similar numerical fit precision. The Fermi velocity is fitted to $v \sim \frac{\pi}{3}$. In the inset the energy difference $E_{1,L} - E_{0,L}$ is plotted vs. $1/L$ and according to Eq. (5) we have fitted the scaling dimension $x = 0.638 \pm 0.0010$. The data points correspond to chains (PBCs) with 30, 60, 90, and 120 sites.

5 Conclusion

To summarize, we have investigated critical spin models of higher representations of SU(2), SU(3) and SU(4) by DMRG, extracting the central charge as well as the scaling dimension of the primary field from our numerical results. These results agree accurately with the predictions of the associated conformal field theories, the SU$(N)_k$ WZW models. We have thus shown that the study of block entropies within DMRG is a suitable numerical tool to investigate SU(N) spin chains including higher representations. It thus represents a fruitful method to complement analytical approaches to these models and perspectively provide important information on models where analytical methods may not be practicable or even applicable.

Acknowledgements We thank D. Schuricht for useful discussions and a critical reading of the manuscript. SR is supported by the Cusanuswerk, RT by the Studienstiftung des deutschen Volkes. MG and PS are supported by the Deutsche Forschungsgemeinschaft (DFG) through grant FOR 960.

A Gell–Mann matrices for the fundamental representation 3 of SU(3)

The algebra su(3) has two diagonal generators V^3 and V^8. The SU(3) Gell-Mann matrices for the fundamental representation are given by [15]

$$V^1 = \begin{pmatrix} 0 & 1 & 0 \\ 1 & 0 & 0 \\ 0 & 0 & 0 \end{pmatrix}, \qquad V^2 = \begin{pmatrix} 0 & -i & 0 \\ i & 0 & 0 \\ 0 & 0 & 0 \end{pmatrix}, \qquad V^3 = \begin{pmatrix} 1 & 0 & 0 \\ 0 & -1 & 0 \\ 0 & 0 & 0 \end{pmatrix},$$

$$V^4 = \begin{pmatrix} 0 & 0 & 1 \\ 0 & 0 & 0 \\ 1 & 0 & 0 \end{pmatrix}, \qquad V^5 = \begin{pmatrix} 0 & 0 & -i \\ 0 & 0 & 0 \\ i & 0 & 0 \end{pmatrix}, \qquad V^6 = \begin{pmatrix} 0 & 0 & 0 \\ 0 & 0 & 1 \\ 0 & 1 & 0 \end{pmatrix},$$

$$V^7 = \begin{pmatrix} 0 & 0 & 0 \\ 0 & 0 & -i \\ 0 & i & 0 \end{pmatrix}, \qquad V^8 = \frac{1}{\sqrt{3}} \begin{pmatrix} 1 & 0 & 0 \\ 0 & 1 & 0 \\ 0 & 0 & -2 \end{pmatrix}.$$

They are normalized as $\mathrm{tr}\left(V^a V^b\right) = 2\delta_{ab}$ and satisfy the commutation relations $\left[V^a, V^b\right] = 2f^{abc}V^c$. The structure constants f^{abc} are totally antisymmetric and obey Jacobi's identity

$$f^{abc}f^{cde} + f^{bdc}f^{cae} + f^{dac}f^{cbe} = 0.$$

Explicitly, the non-vanishing structure constants are given by $f^{123} = i$, $f^{147} = f^{246} = f^{257} = f^{345} = -f^{156} = -f^{367} = i/2$, $f^{458} = f^{678} = i\sqrt{3}/2$, and 45 others obtained by permutations of the indices.

B Matrices for the representation 6 of SU(3)

For completeness, we write out the matrix representation of the SU(3) generators for representation **6**, as those are rarely given explicitly in the literature. As illustrated in Fig 1b (or also from the Gell–Mann matrices above), su(3) possesses two diagonal generators J^3 and J^8 and 6 ladder operators, where always pairs like I^+, I^- are adjoint counterparts or hermitian conjugates of each other. In the notation of Eq. (9), $J^3_{\text{rep.6}}$ corresponds to S^3 and likewise $J^8_{\text{rep.6}} \equiv S^8$. The ladder operators are connected to the spin operators

by $S^1 \pm iS^2 = I^{\pm}$, $S^4 \pm iS^5 = U^{\pm}$, and $S^6 \pm iS^7 = V^{\pm}$. In the following, dots denote zeroes:

$$J^3_{\text{rep.6}} = \begin{pmatrix} 1 & \cdot & \cdot & \cdot & \cdot & \cdot \\ \cdot & \cdot & \cdot & \cdot & \cdot & \cdot \\ \cdot & \cdot & -1 & \cdot & \cdot & \cdot \\ \cdot & \cdot & \cdot & \frac{1}{2} & \cdot & \cdot \\ \cdot & \cdot & \cdot & \cdot & \frac{-1}{2} & \cdot \\ \cdot & \cdot & \cdot & \cdot & \cdot & \cdot \end{pmatrix}, \quad J^8_{\text{rep.6}} = \begin{pmatrix} \frac{1}{\sqrt{3}} & \cdot & \cdot & \cdot & \cdot & \cdot \\ \cdot & \frac{1}{\sqrt{3}} & \cdot & \cdot & \cdot & \cdot \\ \cdot & \cdot & \frac{1}{\sqrt{3}} & \cdot & \cdot & \cdot \\ \cdot & \cdot & \cdot & \frac{-1}{2\sqrt{3}} & \cdot & \cdot \\ \cdot & \cdot & \cdot & \cdot & \frac{-1}{2\sqrt{3}} & \cdot \\ \cdot & \cdot & \cdot & \cdot & \cdot & \frac{-2}{\sqrt{3}} \end{pmatrix},$$

$$I^+_{\text{rep.6}} = \begin{pmatrix} \cdot & \sqrt{2} & \cdot & \cdot & \cdot & \cdot \\ \cdot & \cdot & \sqrt{2} & \cdot & \cdot & \cdot \\ \cdot & \cdot & \cdot & \cdot & \cdot & \cdot \\ \cdot & \cdot & \cdot & \cdot & 1 & \cdot \\ \cdot & \cdot & \cdot & \cdot & \cdot & \cdot \\ \cdot & \cdot & \cdot & \cdot & \cdot & \cdot \end{pmatrix}, \quad V^+_{\text{rep.6}} = \begin{pmatrix} \cdot & \cdot & \cdot & \sqrt{2} & \cdot & \cdot \\ \cdot & \cdot & \cdot & \cdot & 1 & \cdot \\ \cdot & \cdot & \cdot & \cdot & \cdot & \cdot \\ \cdot & \cdot & \cdot & \cdot & \cdot & \sqrt{2} \\ \cdot & \cdot & \cdot & \cdot & \cdot & \cdot \\ \cdot & \cdot & \cdot & \cdot & \cdot & \cdot \end{pmatrix},$$

$$U^+_{\text{rep.6}} = \begin{pmatrix} \cdot & \cdot & \cdot & \cdot & \cdot & \cdot \\ \cdot & \cdot & \cdot & 1 & \cdot & \cdot \\ \cdot & \cdot & \cdot & \cdot & \sqrt{2} & \cdot \\ \cdot & \cdot & \cdot & \cdot & \cdot & \cdot \\ \cdot & \cdot & \cdot & \cdot & \cdot & \sqrt{2} \\ \cdot & \cdot & \cdot & \cdot & \cdot & \cdot \end{pmatrix}.$$

C Matrices for the fundamental representation 4 of SU(4)

su(4) has three diagonal generators V^3, V^8, and V^{15}. The matrices for the fundamental representation of SU(4) are given by:

$$V^1 = \begin{pmatrix} 0 & 1 & 0 & 0 \\ 1 & 0 & 0 & 0 \\ 0 & 0 & 0 & 0 \\ 0 & 0 & 0 & 0 \end{pmatrix}, \quad V^2 = \begin{pmatrix} 0 & -i & 0 & 0 \\ i & 0 & 0 & 0 \\ 0 & 0 & 0 & 0 \\ 0 & 0 & 0 & 0 \end{pmatrix}, \quad V^3 = \begin{pmatrix} 1 & 0 & 0 & 0 \\ 0 & -1 & 0 & 0 \\ 0 & 0 & 0 & 0 \\ 0 & 0 & 0 & 0 \end{pmatrix},$$

$$V^4 = \begin{pmatrix} 0 & 0 & 1 & 0 \\ 0 & 0 & 0 & 0 \\ 1 & 0 & 0 & 0 \\ 0 & 0 & 0 & 0 \end{pmatrix}, \quad V^5 = \begin{pmatrix} 0 & 0 & -i & 0 \\ 0 & 0 & 0 & 0 \\ i & 0 & 0 & 0 \\ 0 & 0 & 0 & 0 \end{pmatrix}, \quad V^6 = \begin{pmatrix} 0 & 0 & 0 & 0 \\ 0 & 0 & 1 & 0 \\ 0 & 1 & 0 & 0 \\ 0 & 0 & 0 & 0 \end{pmatrix},$$

$$V^7 = \begin{pmatrix} 0 & 0 & 0 & 0 \\ 0 & 0 & -i & 0 \\ 0 & i & 0 & 0 \\ 0 & 0 & 0 & 0 \end{pmatrix}, \quad V^8 = \frac{1}{\sqrt{3}} \begin{pmatrix} 1 & 0 & 0 & 0 \\ 0 & 1 & 0 & 0 \\ 0 & 0 & -2 & 0 \\ 0 & 0 & 0 & 0 \end{pmatrix}, \quad V^9 = \begin{pmatrix} 0 & 0 & 0 & 1 \\ 0 & 0 & 0 & 0 \\ 0 & 0 & 0 & 0 \\ 1 & 0 & 0 & 0 \end{pmatrix},$$

$$V^{10} = \begin{pmatrix} 0 & 0 & 0 & -i \\ 0 & 0 & 0 & 0 \\ 0 & 0 & 0 & 0 \\ i & 0 & 0 & 0 \end{pmatrix}, \quad V^{11} = \begin{pmatrix} 0 & 0 & 0 & 0 \\ 0 & 0 & 0 & 1 \\ 0 & 0 & 0 & 0 \\ 0 & 1 & 0 & 0 \end{pmatrix}, \quad V^{12} = \begin{pmatrix} 0 & 0 & 0 & 0 \\ 0 & 0 & 0 & -i \\ 0 & 0 & 0 & 0 \\ 0 & i & 0 & 0 \end{pmatrix},$$

$$V^{13} = \begin{pmatrix} 0 & 0 & 0 & 0 \\ 0 & 0 & 0 & 0 \\ 0 & 0 & 0 & 1 \\ 0 & 0 & 1 & 0 \end{pmatrix}, \quad V^{14} = \begin{pmatrix} 0 & 0 & 0 & 0 \\ 0 & 0 & 0 & 0 \\ 0 & 0 & 0 & -i \\ 0 & 0 & i & 0 \end{pmatrix}, \quad V^{15} = \frac{1}{\sqrt{6}} \begin{pmatrix} 1 & 0 & 0 & 0 \\ 0 & 1 & 0 & 0 \\ 0 & 0 & 1 & 0 \\ 0 & 0 & 0 & -3 \end{pmatrix}.$$

References

[1] E. Schrödinger, Annalen der Physik **81**, 109 (1926).
[2] W. Heisenberg, Z. Phys. **43**, 172 (1927).
[3] H. Bethe, Z. Phys. **71**, 205 (1931), translated in: The Many-Body Problem, edited by D.C. Mattis (World Scientific, Singapore, 1993).
[4] C.N. Yang, Phys. Rev. Lett. **19**, 1312 (1967).
[5] L. Faddeev, in: Recent Advances in Field Theory and Statistical Mechanics, Les Houches Lectures, Vol. 39, edited by J.-B. Zuber and R. Stora (Elsevier, Amsterdam, 1982).
[6] V.E. Korepin, N.M. Bogoliubov, and A.G. Izergin, Quantum Inverse Scattering Method and Correlation Functions (Cambridge University Press, Cambridge, 1997).
[7] L.D. Faddeev and L.A. Takhtajan, Phys. Lett. A **85**, 375 (1981).
[8] F.D.M. Haldane, Phys. Lett. A **93**, 464 (1983).
[9] F.D.M. Haldane, Phys. Rev. Lett. **50**, 1153 (1983).
[10] I. Affleck, in: Fields, Strings and Critical Phenomena, Les Houches Lectures, Vol. 49, edited by E. Brézin and J. Zinn-Justin (Elsevier, Amsterdam, 1990).
[11] E. Fradkin, Field Theories of Condensed Matter Systems, Frontiers in Physics 82 (Westview Press, Bouler, 1991).
[12] W.J.L. Buyers, R.M. Morra, R.L. Armstrong, M.J. Hogan, P. Gerlach, and K. Hirakawa, Phys. Rev. Lett. **56**, 371 (1986).
[13] J.P. Renard, M. Verdaguer, L.P. Regnault, W.A.C. Erkelens, J. Rossat-Mignod, and W.G. Stirling, Europhys. Lett. **3**, 945 (1987).
[14] S. Ma, C. Broholm, D.H. Reich, B.J. Sternlieb, and R.W. Erwin, Phys. Rev. Lett. **69**, 3571 (1992).
[15] J.F. Cornwell, Group Theory in Physics, Vol. 2 (Academic Press, London, 1984).
[16] M. Greiter and S. Rachel, Phys. Rev. B **75**, 184441 (2007).
[17] S. Capponi, G. Roux, P. Lecheminant, P. Azaria, E. Boulat, and S.R. White, Phys. Rev. A **77**, 013624 (2008).
[18] Y.Q. Li, M. Ma, D.N. Shi, and F.C. Zhang, Phys. Rev. B **60**, 12781 (1999).
[19] S.J. Gu and Y.Q. Li, Phys. Rev. B **66**, 092404 (2002).
[20] I. Affleck and F.D.M. Haldane, Phys. Rev. B **36**, 5291 (1987).
[21] I. Affleck, Nucl. Phys. B **305**, 582 (1988).
[22] I. Affleck, Nucl. Phys. B **265**, 409 (1986).
[23] P. Di Francesco, P. Mathieu, and D. Sénéchal, Conformal Field Theory (Springer, New York, 1997).
[24] J. Wess and B. Zumino, Phys. Lett. **37B**, 95 (1971).
[25] E. Witten, Commun. Math. Phys. **92**, 455 (1984).

[26] S. R. White, Phys. Rev. Lett. **69**, 2863 (1992).
[27] U. Schollwöck, Rev. Mod. Phys. **77**, 259 (2005).
[28] R. M. Noack and S. R. Manmana, in: Diagonalization- und Numerical Renormalization-Group-Based Methods for Interacting Quantum Systems, AIP Conference Proceedings 789 (AIP, Melville, NY, 2005), p. 93.
[29] K. Hallberg, Adv. Phys. **55**, 477 (2006).
[30] L. A. Takhtajan, Phys. Lett. **87A**, 479 (1982).
[31] H. M. Babudjan, Phys. Lett. **90A**, 479 (1982).
[32] H. M. Babudjan, Nucl. Phys. B **215**, 317 (1983).
[33] N. Andrei and H. Johannesson, Phys. Lett. **104A**, 370 (1984).
[34] H. Johannesson, Nucl. Phys. B **270**, 235 (1986).
[35] V. E. Korepin, Phys. Rev. Lett. **92**, 096402 (2004).
[36] P. Calabrese and J. Cardy, J. Stat. Mech. **P06002** (2004).
[37] J. L. Cardy, J. Phys. A, Math. Gen. **17**, L385 (1984).
[38] I. Affleck, D. Gepner, H. J. Schulz, and T. Ziman, J. Phys. A, Math. Gen. **22**, 511 (1989).
[39] P. Corboz, A. M. Läuchli, K. Totsuka, and H. Tsunetsugu, Phys. Rev. B **76**, 220404(R) (2007).
[40] B. Sutherland, Phys. Rev. B **12**, 3795 (1975).
[41] F. C. Alcaraz and M. J. Martins, J. Phys. A, Math. Gen. **21**, 4397 (1988).
[42] F. C. Alcaraz and M. J. Martins, J. Phys. A, Math. Gen. **22**, L865 (1989).
[43] M. J. Martins, Phys. Rev. Lett. **65**, 2091 (1990).
[44] R. Molina and P. Schmitteckert, Phys. Rev. B **75**, 235104 (2007).
[45] P. Schmitteckert and R. Werner, Phys. Rev. B **69**, 195115 (2004).
[46] I. P. McCulloch and M. Gulácsi, Europhys. Lett. **57**, 852 (2002).
[47] J. L. Cardy, J. Phys. A, Math. Gen. **19**, 1093 (1986).
[48] K. Hijii and K. Nomura, Phys. Rev. B **65**, 104413 (2002).

